



# A fast permeability measurement method based on congenetic bilateral pulse decay

Mingbao Zhang<sup>1</sup>, Yue Wang<sup>1</sup>, Zhiguo Tian, Moran Wang<sup>\*</sup>

Department of Engineering Mechanics, Tsinghua University, Beijing, 100084, China

## ARTICLE INFO

### Keywords:

Pulse-decay method  
Porous media  
Permeability  
Bilateral pulse

## ABSTRACT

The pulse-decay method is a transient approach widely employed for permeability measurements, holding significant relevance for modeling and utilizing flow in low permeable porous media. Most of the existing pulse-decay methods predominantly rely on pressurization or depressurization in one chamber, requiring gas penetration through the entire sample and complete attenuation, which may take a long time for ultra-low-permeability materials. This study proposes the congenetic bilateral pulse-decay method by utilizing a bypass conduit to achieve bilateral pulses to accelerate the measurement process. The mathematical and physical modeling along with the realistic experimental conditions leads to more concise analytical solutions and permeability calculation methods. Comparisons of measurement duration and sensitivity between the present method and the previous pulse-decay methods show that this new method achieves an efficiency improvement of at least four times while maintaining the simultaneity and symmetry of bilateral pulse with a straightforward and cost-effective experimental setup. This measurement method may further reduce the measurement time and costs in permeability measurements of ultra-low permeable porous media.

## 1. Introduction

Permeability is a critical parameter that characterizes the ability of fluids to flow through porous media under the influence of a pressure gradient. In the realm of low-permeability rock formation, such as unconventional reservoirs (shale, etc),<sup>1,2</sup> disposal of nuclear waste,<sup>3,4</sup> carbon dioxide sequestration,<sup>5-7</sup> and others, accurate measurement of low permeability is a crucial prerequisite for ensuring the successful implementation and stable operation of various technologies. There are two primary methods for laboratory measurements of rock permeability: steady-state and transient methods.<sup>8-12</sup> For tight and low-permeability rock samples, where the steady-state method takes a long time to measure and the flow rate is not easy to measure, the transient method is considered to be more applicable.<sup>13-17</sup> For example, for shale samples with permeability around 0.4nD, the steady state method requires continuous measurements for more than 170h to obtain stable results, and the transient method requires about 20h.<sup>13</sup>

The pulse decay method is one of the most popular transient measurement techniques,<sup>18-20</sup> which was initially proposed by Brace et al.<sup>21</sup> The typical experimental setup primarily consists of a sample holder,

two finite-volume chambers, pressure gauges, and connecting pipes. During the experiment, the pressure pulses are applied at one chamber, and the pressure evolution at both chambers are measured and recorded to calculate the permeability.<sup>22,23</sup> Over the ensuing decades, a multitude of scholars have endeavored to enhance the pulse decay method through the utilization of diverse experimental designs aimed at further reducing measurement time.<sup>9,15,24-27</sup> In some methods, the downstream side is directly exposed to the atmosphere, with the pressure consistently maintained at the atmospheric level, and the permeability is exclusively calculated based on the pressure drop within the upstream chamber.<sup>28,29</sup> Similarly, the upstream pressure can also be held at a constant level,<sup>30-33</sup> with the permeability calculated based on the pressure rise of the downstream chamber. On the other hand, one end of the sample can be sealed using a metal disk, so that only one single chamber and one pressure gauge are required, resulting in a more compact experimental configuration,<sup>34,35</sup> and this setup yields a shorter measurement time. By solving the pulse decay process, permeability can be calculated through the logarithmic pressure difference -time ( $\ln \Delta P$  vs.  $t$ ) curve. Previous studies have shown that the boundary conditions correspond to the configuration of the two end chambers in the experiment, determining the slope of the late-stage curve and simultaneously affecting the

\* Corresponding author.

E-mail address: [mrwang@tsinghua.edu.cn](mailto:mrwang@tsinghua.edu.cn) (M. Wang).

<sup>1</sup> MZ and YW contribute equally to this work.

**Symbols list:**

$A$	Cross-sectional area of the sample
$b_s$	Slip coefficient
$f$	Intercept
$k_{app}$	Apparent permeability
$k_{int}$	Intrinsic permeability
$L$	Length of the sample
$P$	Pore pressure
$P_D$	Dimensionless pressure
$P_d(0)$	Initial downstream pressure
$P_u(0)$	Initial upstream pressure
$P_u(t)$	Upstream pressure
$P_d(t)$	Downstream pressure
$R^2$	Fitting correlation coefficient
$s$	Sensitivity
$t$	Temporal coordinate

$t_D$	Dimensionless temporal coordinate
$V_u$	Volume of the upstream chamber
$V_{uD}$	Dimensionless upstream volume
$V_d$	Volume of the downstream chamber
$V_{dD}$	Dimensionless downstream volume
$x$	Spatial coordinate
$x_D$	Dimensionless spatial coordinate

*Greek letter*

$\alpha$	Slope
$\beta_\rho$	Gas compressibility factor
$\Gamma$	Test duration
$\theta_m$	m-th non-negative root
$\mu$	Fluid dynamic viscosity
$\rho$	Fluid density
$\varphi$	Porosity

intercept. Initial conditions correspond to the method of pulse application, influencing only the intercept. Through analysis of various approaches, it has been determined that applying pulses to chambers with smaller volumes is an effective strategy for reducing measurement time. Therefore, the unilateral sealing method exhibits the highest measurement speed.<sup>10</sup> Nevertheless, in all of the aforementioned experimental procedures, a pressure pulse has to be applied by pressurizing or depressurizing a single chamber, and the measurement can be completed only after the pulse permeating the entire sample, which may take a quite long time, especially for ultra-low-permeability porous media.

To reduce the measurement time, it is natural and straightforward to apply two pressure pulses on both sides of the sample. Initially, a bilateral pressurization was employed for gas injection to achieve pressure equilibrium, essentially remaining within the realm of the unilateral pulse method, with pressure applied on both sides primarily for measuring bidirectional permeability.<sup>36</sup> Subsequently, Hannon proposed a bilateral-pulse design with two pulses applied severally on two sides of the sample and reported a remarkable acceleration in measurement compared to single-pulse-decay experiments with same conditions elsewhere.<sup>37</sup> The design is attractive and promising, while reliable validations are still demanded but lacking. Furthermore, some researchers attempted to pressurize the upstream chamber while simultaneously depressurizing the downstream chamber by the same magnitude, striving to maintain equal chamber volumes of two sides to ensure consistent average pressure within the system throughout the testing process.<sup>38</sup> The achievement was reached to eliminate the impacts of compression storage and adsorption effects on permeability measurements, but it hurt the efforts of reducing the measurement time.

This study proposes a congenetic bilateral pulse-decay method utilizing a bypass conduit between the upstream and downstream sides to apply congenetic pulses on both sides of the sample simultaneously. In light of the aforementioned issues and objectives, this work is organized into the following sections: In Sec. 2, a detailed description of the experimental apparatus and procedures is provided. In Sec. 3, a comprehensive mathematical model is developed, incorporating new boundary conditions based on experimental conditions, and analytical solutions are obtained. In Sec. 4, the feasibility of this method is validated through experiments compared to conventional pulse decay methods. In Sec. 5, a comprehensive evaluation of this method is carried out, considering both measurement duration and accuracy. Finally, conclusions are presented in Sec. 6.

## 2. Experiment design

The experimental design for the proposed congenetic bilateral pulse method in this study necessitates only minor adjustments to the prevailing experimental framework, which employs finite-volume chambers on both sides. Fig. 1 presents a schematic diagram of the experimental setup specific to the bilateral pulse method. Similar to the experimental configuration introduced by Brace et al.,<sup>21</sup> the congenetic bilateral pulse method also incorporates two finite-volume chambers on either side of the sample. The distinguishing feature lies in the incorporation of a bypass conduit, establishing a direct connection between the upstream and downstream chambers. When the valve on the bypass conduit is closed, this setup reverts to the experimental apparatus corresponding to the finite-volume chambers on both ends.

The experimental procedure for the congenetic bilateral pulse method encompasses the following sequential stages.

- (1) The porous media sample is meticulously prepared and positioned within the sample holder. The ends of the sample are securely connected to the upstream and downstream gas chambers via pipelines, and the sides of the sample are meticulously sealed using metal foil and sleeves. Porous steel disks are strategically placed at both ends of the sample to ensure uniform flow. Perform seal integrity inspection using appropriate methods (e.g., soap bubble method). Subsequently, the entire apparatus is placed in an oven to maintain a constant temperature.
- (2) By pressurizing the liquid between the rubber sleeve and the metal casing, a specified confining pressure is carefully applied to the sample. The test gas is then introduced into the apparatus, and the valves between the two chambers and the sample holder are opened. The system is allowed to equilibrate until the pressures in the upstream and downstream chambers are equal, thereby establishing the initial equilibrium pressure denoted as  $P_d(0)$  as shown in Fig. 2(a).
- (3) The bypass valve connecting the upstream and downstream chambers is opened, and the valves between the chambers and the sample holder are closed. High-pressure gas is injected into the upstream chamber from a pressurized gas cylinder, elevating the upstream pressure to the designated value, which is termed the initial upstream pressure  $P_u(0)$  as shown in Fig. 2(b).
- (4) The valves between the upstream and downstream chambers and the sample holder are opened. Gas begins to flow concurrently into the sample from the upstream and downstream chambers, propelled by the pressure differential. Simultaneously, continuous monitoring is conducted to record the pressure changes

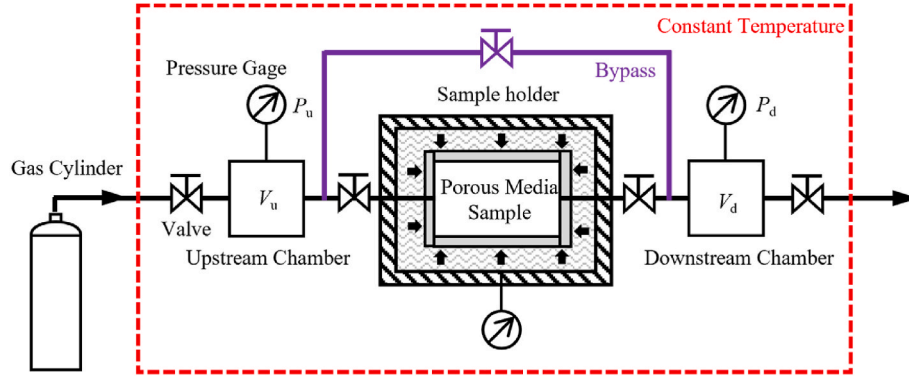


Fig. 1. Schematic diagram of the experimental setup for the congenetic bilateral pulse method. The bypass conduit provides a direct connection between the upstream and downstream chambers and can be closed.

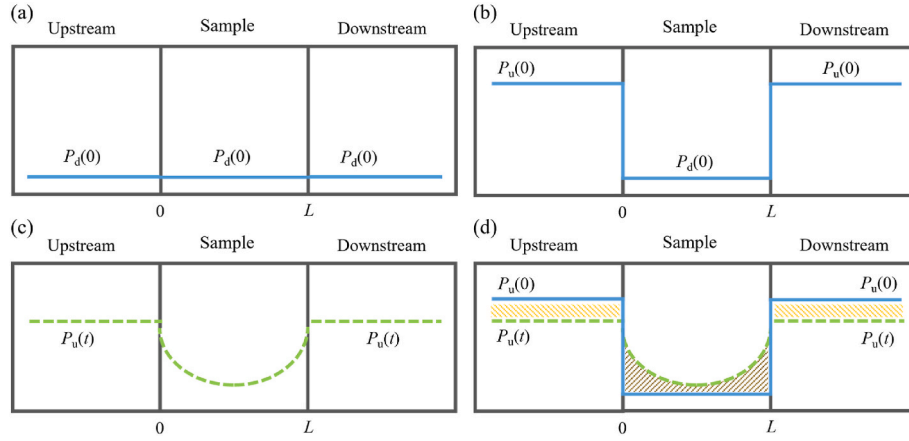


Fig. 2. Schematic diagram of pressure variation in the measurement process by the bilateral pulse method: (a) Initial equilibrium pressure profile; (b) Initial pressure profile after pressurization of the upstream and downstream chambers; (c) Pressure profile during pulse decay process; (d) Comparison of pressure profile changes during initial and decay processes.

within the upstream and downstream pressure chambers over time, represented as  $P_u(t)$ . The pressure profile during this process is displayed in Fig. 2(c) and the comparison with the initial pressure condition is displayed in Fig. 2(d).

It is worth addressing that while the initial pulse is applied by pressurizing the upstream chamber through gas injection, the presence of the bypass conduit guarantees the synchronization of downstream chamber pressure with the upstream pressure, resulting in the achievement of concurrent bilateral pulses. Furthermore, in comparison to the previous experimental configuration,<sup>37</sup> the cost of pipelines and connecting screws is significantly lower than that of precision pressure supply and detection devices, highlighting the cost-saving advantage of this method. As illustrated in Fig. 2, throughout the measurement process, the porous media sample exhibits significantly higher flow resistance in comparison to the bypass conduit. This ensures that even if the volumes of the upstream and downstream chambers are not perfectly matched, the pressures in both the upstream and downstream chambers remain in equilibrium. Gas simultaneously flows into the sample from both ends of the chambers, ensuring the symmetry of the bilateral pulse, which is an advantage over applying pulses separately on both sides.

### 3. Process analysis

Modeling and analyzing the measurement process in the bilateral pulse method is a prerequisite for calculating permeability. Assuming that at the initial moment, the pressure difference between the upstream

and downstream is extremely small, and the porous media sample is homogeneous, this process can still be described using the linear control equation derived by Brace et al. for the pulse decay process:

$$\frac{\partial P}{\partial t} = \frac{k_{app}}{\beta_p \mu \varphi} \frac{\partial^2 P}{\partial x^2}, \quad (1)$$

where  $P$  [Pa] represents fluid pressure, also known as pore pressure,  $k_{app}$  [m<sup>2</sup>] is the apparent permeability,  $\mu$  [Pa·s] is the fluid dynamic viscosity,  $\beta_p = \frac{d \ln \rho}{d \ln P}$  [Pa<sup>-1</sup>] is the gas compressibility factor,  $\rho$  [kg·m<sup>-3</sup>] is the fluid density,  $\varphi$  is the porosity of the sample,  $x$  [m] and  $t$  [s] are the spatial and temporal coordinates, respectively. This linear equation applies when the relative pressure difference between the samples is less than 10 %, and for bilateral pulses it applies when the pulse pressure is less than 10 % of the equilibrium pressure.<sup>14,15,39–42</sup> In the congenetic bilateral pulse method, the linkage between the upstream and downstream chambers via a bypass conduit maintains equilibrium in pressure at both ends of the porous media sample. According to the principle of mass conservation, the mass of gas entering the porous media sample equals the mass of gas exiting from both chambers. Therefore, under minor pressure difference conditions, the boundary conditions in the bilateral pulse method can be concisely articulated as follows:

$$\frac{\partial P}{\partial t} \Big|_{x=0} = \frac{k_{app} A}{\beta_p \mu (V_u + V_d)} \left( \frac{\partial P}{\partial x} \Big|_{x=0} - \frac{\partial P}{\partial x} \Big|_{x=L} \right), P(0, t) = P(L, t), \quad (2)$$

where  $L$  [m] and  $A$  [m<sup>2</sup>] represent the length and cross-sectional area of the sample,  $V_u$  [m<sup>3</sup>] and  $V_d$  [m<sup>3</sup>] are the volumes of the upstream and

downstream chambers, respectively. When contrasting the boundary conditions of the bilateral pulse method with those of the conventional unilateral pulse method, in situations where the upstream and downstream chambers are not interlinked, the alteration in pressure on one side of the sample is solely contingent on the local pressure gradient. In contrast, the bilateral pulse approach dictates that the pressure variation on each side of the sample is concomitantly shaped by the pressure gradients at both ends of the sample. Assuming that the initial pressure pulse is applied by pressurizing the chambers, the initial conditions can be expressed as:

$$P(x, 0) = \begin{cases} P_u(0), x = 0, L \\ P_d(0), 0 < x < L \end{cases}, \quad (3)$$

where  $P_u(0)$  [Pa] and  $P_d(0)$  [Pa] represent the pressure values inside the upstream and downstream chambers when the pulse is applied. Choosing the sample length  $L$  as the characteristic length, and based on the governing equation (1), the characteristic time for the pulse decay process is  $\beta_\rho \mu \phi L^2 / k_{app}$ . Therefore, dimensionless spatial position and non-dimensional time can be defined as:

$$x_D = \frac{x}{L}, t_D = \frac{k_{app} t}{\beta_\rho \mu \phi L^2}. \quad (4)$$

The dimensionless (excess) pressure can be defined as:

$$P_D(x_D, t_D) = \frac{P(x_D, t_D) - P_d(0)}{P_u(0) - P_d(0)}. \quad (5)$$

Using the aforementioned dimensionless parameters, the governing equation (1) can be rewritten in dimensionless form as:

$$\frac{\partial P_D}{\partial t_D} = \frac{\partial^2 P_D}{\partial x_D^2}. \quad (6)$$

The dimensionless boundary and initial conditions can be expressed as:

$$\left. \frac{\partial P_D}{\partial t_D} \right|_{x_D=0} = \frac{V_{uD} V_{dD}}{V_{uD} + V_{dD}} \left( \left. \frac{\partial P_D}{\partial x_D} \right|_{x_D=0} - \left. \frac{\partial P_D}{\partial x_D} \right|_{x_D=1} \right), P_D(0, t_D) = P_D(1, t_D), \quad (7)$$

$$P_D(x_D, 0) = \begin{cases} 1, x_D = 0, 1 \\ 0, 0 < x_D < 1 \end{cases}, \quad (8)$$

where  $V_{uD}$  and  $V_{dD}$  represent the ratios of the sample pore volume to the volumes of the upstream and downstream chambers, respectively:

$$V_{uD} = \frac{LA\phi}{V_u}, V_{dD} = \frac{LA\phi}{V_d}. \quad (9)$$

Combining equation (6) (7) and (8), the bilateral pulse process can be analytically solved. Employing the method of separation of variables to decompose  $P_D(x_D, t_D)$  into a product form and substituting it into the governing equation and boundary conditions, the eigenfunction set  $\{X_m\}$  can be obtained. Expressing the initial conditions as an expansion using the eigenfunction set as a basis, the solution for the bilateral pulse process is then given by:

$$P_D(x_D, t_D) = \frac{V_{uD} V_{dD}}{V_{uD} V_{dD} + V_{uD} + V_{dD}} + 2 \sum_{m=1}^{+\infty} \frac{\theta_m \sin(\theta_m x_D) - V_{uD} \cos(\theta_m x_D)}{\sin \theta_m - \theta_m} \exp(-\theta_m^2 t_D), \quad (10)$$

where  $\theta_m$  is the  $m$ -th non-negative root of the following transcendental equation:

$$\tan\left(\frac{\theta_m}{2}\right) = -\frac{V_{uD} + V_{dD}}{V_{uD} V_{dD}} \frac{\theta_m}{2}. \quad (11)$$

Although both volume ratios  $V_{uD}$  and  $V_{dD}$  appear simultaneously in

equation (10), it can be collated to show that actually  $\theta_m$  is only a function of  $V_{uD} V_{dD} / (V_{uD} + V_{dD})$ , which is actually the ratio of the sample pore volume to the sum of the upstream and downstream chambers:

$$\frac{V_{uD} V_{dD}}{V_{uD} + V_{dD}} = \frac{LA\phi}{V_u + V_d}. \quad (12)$$

In existing experimental setups, changing the volume of either chamber can affect the solution of the pulse decay process.<sup>37</sup> The congenetic bilateral pulse method in this work, where both side chambers are interconnected, results in the pivotal factor being the combined volume of the bilateral chambers rather than the volume of a single side. As shown in Fig. 3, under the condition of keeping the total volume constant, only changing the relative sizes of the chambers at both ends results in pressure change curves that overlap with each other.

In practical measurements, only the pressure values in the upstream and downstream chambers can be measured. Setting  $x_D = 0$  or  $x_D = 1$  in equation (10), the expressions for the upstream or downstream pressure can be obtained as:

$$P_{uD}(t_D) = P_{dD}(t_D) = \frac{V_{uD} V_{dD}}{V_{uD} V_{dD} + V_{uD} + V_{dD}} + 2 \sum_{m=1}^{+\infty} \frac{\sin(\theta_m)}{\sin \theta_m - \theta_m} \exp(-\theta_m^2 t_D). \quad (13)$$

From equation (13), similar to other experimental schemes, the solution of pressure in the congenetic bilateral pulse scheme is still composed of a set of exponential functions with different decay rates. Therefore, for sufficiently large time  $t_D$ , a late-time solution can be expressed:

$$P_{uD}(t_D) = P_{dD}(t_D) \approx \frac{V_{uD} V_{dD}}{V_{uD} V_{dD} + V_{uD} + V_{dD}} + \frac{2 \sin(\theta_1)}{\sin \theta_1 - \theta_1} \exp(-\theta_1^2 t_D). \quad (14)$$

The late-time solution typically consists of a constant term and an exponential term. Hannon's analytical solution,<sup>37</sup> which involves applying pulses separately on both sides, requires considering the relative size of the upstream and downstream chambers, making it more complex compared to the results presented in this study. In experimental setups with finite volumes in both chambers or with one side maintaining constant pressure, a direct difference between the upstream and downstream pressures eliminates the constant term, leaving only the exponential term. Therefore, the logarithm of the upstream-downstream pressure difference will linearly decay with time in the late stage, and its

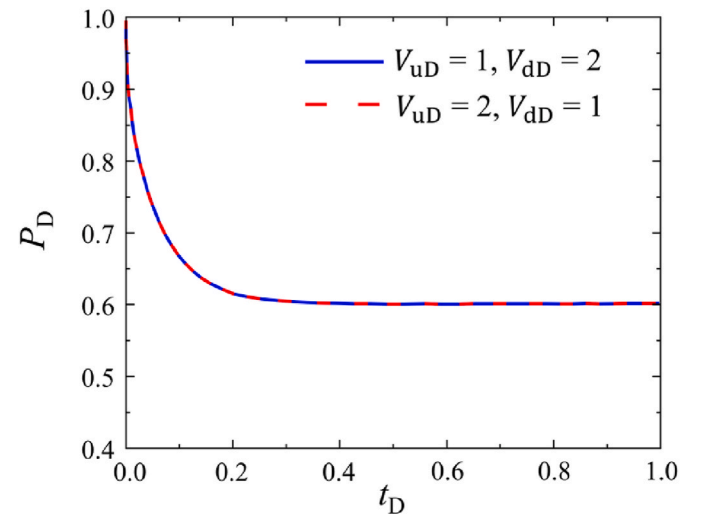


Fig. 3. Pressure change curves in the upstream and downstream chambers. Different values of  $V_{uD}$  and  $V_{dD}$  represent different volume ratios in the upstream and downstream.

decay rate can be used to calculate the sample permeability. However, in the bilateral pulse method, despite the capability to connect pressure gauges to both upstream and downstream chambers, the presence of the bypass ensures that the upstream and downstream pressures perpetually remain identical, leading to a null pressure differential on either side of the sample. One approach to address this issue, following the attainment of the system's ultimate equilibrium, involves using the difference between the upstream pressure and the equilibrium pressure as follows:

$$\Delta P_D = P_{UD}(t_D) - P_{UD}(\infty) \approx \frac{2 \sin(\theta_1)}{\sin \theta_1 - \theta_1} \exp(-\theta_1^2 t_D), \quad (15)$$

where " $\infty$ " represents the final equilibrium state. Therefore, in the  $\ln \Delta P_D$  vs.  $t$  chart, a straight line can still be obtained in the late stage. The expression for the slope of this line is the same as that for the lateral pulse case:

$$\alpha = -\frac{\theta_1^2 k_{app}}{\beta_\rho \mu \phi L^2}. \quad (16)$$

The expression for the linear intercept is:

$$f = \ln \frac{2 \sin \theta_1}{\sin \theta_1 - \theta_1}. \quad (17)$$

Hence, with the slope value determined, the sample's permeability can be calculated as follows:

$$k_{app} = -\frac{\alpha \beta_\rho \mu \phi L^2}{\theta_1^2}. \quad (18)$$

#### 4. Experimental Validation

To validate the feasibility of the proposed method, the bilateral pulse experiments are conducted and compared with the conventional unilateral pulse decay method. Considering the gas slippage effect in low-permeability porous media, the Klinkenberg equation is utilized to obtain the intrinsic permeability,  $k_{app} = k_{int}(1 + b_s/P)$ , where  $b_s$  refers to the slip coefficient. Helium gas is utilized as the testing gas due to its stable properties, thus avoiding reactions with the porous samples. Experiments are carried out on shale samples from Eagle Ford under various pore pressures to facilitate Klinkenberg correction. The measurement parameters are summarized in Table 1, and the experimental results are depicted in Fig. 4. In Fig. 4(a), the results obtained using the bilateral pulse method at various pore pressures are presented. It is discernible that, following an initial period, the logarithm of pressure difference exhibits linear decay characteristics. As the pore pressure increases, the rate of pressure decay accelerates. Utilizing the slope in the late stage, the permeability of the sample can be determined. Fig. 4 (b) illustrates the Klinkenberg plot ( $k_{app}$  vs.  $P^{-1}$ ), where the apparent permeability is plotted against the reciprocal of pore pressure. The experiments using conventional unilateral pulse method with the limited chamber volume method on both sides yielded an intercept of 16.192, a slope of 118.87, and a correlation coefficient ( $R^2$ ) of 0.9993. Meanwhile, experiments utilizing the bilateral pulse method resulted in an intercept of 16.893, a slope of 117.43, and a correlation coefficient ( $R^2$ ) of 0.9972.

**Table 1**  
Experimental parameters for the congenetic bilateral pulse decay method.

Setup	Parameter
Test material	Shale
Test gas	Helium
Sample length (m)	$3.16 \times 10^{-2}$
Sample cross-section area (m <sup>2</sup> )	$1.13 \times 10^{-4}$
Sample porosity (%)	11.50
Confining pressure (Pa)	$3 \times 10^7$
Temperature (°C)	35

Therefore, the experimental data from both methods can be considered to lie on the same line, demonstrating the consistency between the bilateral pulse method and the unilateral pulse method in calculating permeability. Employing linear fitting of both datasets, the intrinsic permeability of the sample is determined to be 16.5 nD, and the slip coefficient is 7.2 MPa. The high fitting coefficient of determination  $R^2$  of 0.99 also demonstrates the consistency between the two methods.

During the experimental process, pressure equilibrium was achieved within the initial 2000 s when employing the bilateral pulse method. For the same sample, even after 10000 s, pressure equilibrium was not reached when using the unilateral pulse method with finite volumes at both ends. Despite the relatively fast measurement speed of the traditional pulse decay method, the congenetic bilateral pulse method still holds a significant speed advantage, offering a better choice for certain demanding scenarios, such as ultra-low permeability porous media.

#### 5. Efficiency and accuracy discussion

##### 5.1. Measurement duration

The measurement duration is a critical metric for evaluating pulse decay experimental schemes. To quantitatively study the duration of pulse decay experiments, a specific experiment termination criterion needs to be established. The pulse decay measurement is considered complete when the dimensionless pressure drop, as defined in this study, satisfies the following conditions:

$$\Delta P_D(\Gamma_{0.05}) = \frac{P_u(\Gamma_{0.05}) - P_u(\infty)}{P_u(0) - P_u(\infty)} = 0.05, \quad (19)$$

where  $\Gamma_{0.05}$  represents the test duration of the pulse decay experiment, with the subscript indicating the defined termination criterion. As analyzed earlier, the late-stage approximate series solution is still applicable in the bilateral pulse method. Therefore, substituting equation (15) into equation (19) and taking the logarithm yields:

$$\ln \Delta P_D(\Gamma_{0.05}) \approx f - \theta_1^2 \Gamma_{0.05} \approx \ln(0.05) = -2.996, \quad (20)$$

where  $f$  and  $-\theta_1^2$  are the intercept and slope, respectively, of the plot of the logarithm of the pressure difference versus dimensionless time ( $\ln \Delta P_D$  vs.  $t_D$ ). Rearranging equation (20) yields the expression for  $\Gamma_{0.05}$ :

$$\Gamma_{0.05} \approx \frac{f + 2.996}{\theta_1^2}. \quad (21)$$

Equation (21) shows that the measurement duration of the bilateral pulse test is only related to three parameters. The constant 2.996 in the numerator depends on the prescribed experimental termination criterion, which will become 4.605 if the dimensionless pressure  $\Delta P_D = 0.01$  is utilized as the termination criterion for the pulse decay test. The measurement duration increases as the critical value of  $\Delta P_D$  in the termination criterion decreases. Fig. 5 demonstrates the magnitude of  $\theta_1$  in the congenetic bilateral pulse method in relation to  $\theta_1$  in other experimental schemes when the upstream and downstream chamber volumes are equal. The results reveal that  $\theta_1$  in the bilateral pulse method is significantly larger than  $\theta_1$  in other experimental methods, resulting in much shorter measurement durations in the bilateral pulse method. Specifically, when the volumes of the chambers on one side are equal,  $\theta_1$  in the bilateral pulse method is twice as much as that in the one-side sealed method. Equation (21) implies that the measurement duration in the congenetic bilateral pulse method is approximately one-fourth of that in the one-end sealed method, theoretically indicating the advantage of the measurement duration in the bilateral pulse method compared to other methods.

Indeed, the bilateral pulse method can be considered as a specialized instance of the one-end sealed method. By its inherent symmetry, the congenetic bilateral pulse method ensures that the pressure gradient at

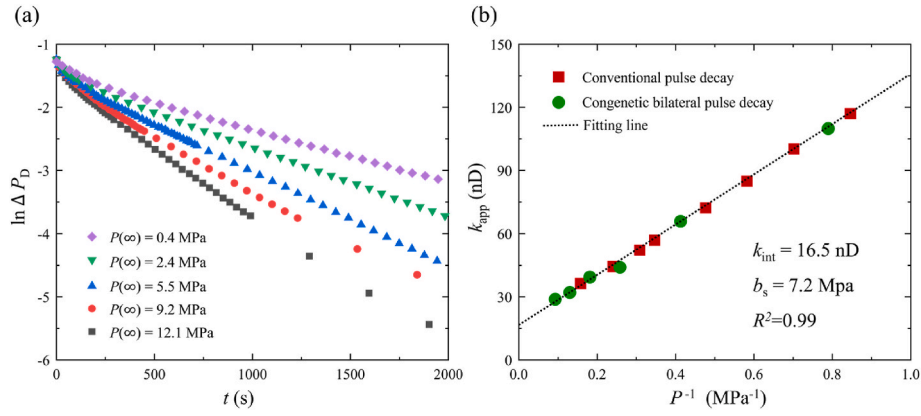


Fig. 4. Experimental result by the congenetic bilateral pulse decay method: (a) Logarithm of pressure difference versus time; (b) Klinkenberg permeability measured by both two experimental methods.

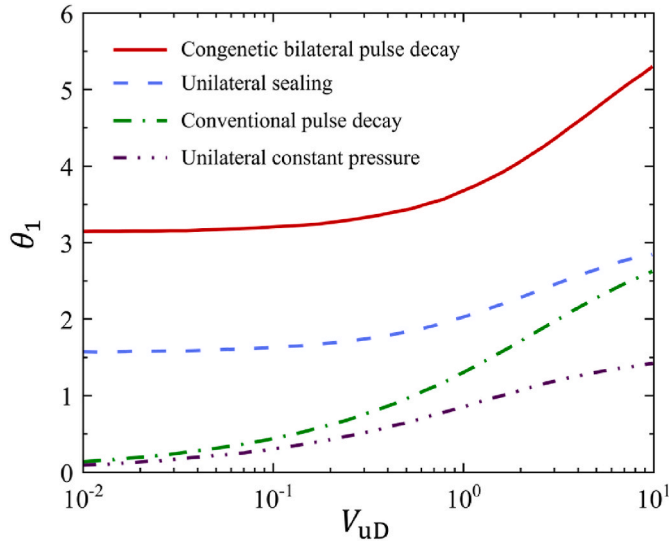


Fig. 5. Comparison of  $\theta_1$  in different experimental schemes. The unilateral sealing represents the closure of the corresponding chamber with zero volume.

the middle cross-section of the sample perpetually remains at a null state. Therefore, the bilateral pulse method can be equivalently regarded as measuring a sample with half the original sample length using a unilateral sealing experimental setup. Previous research has already demonstrated that, when the chamber volumes are equal in the unilateral sealing method, it is the fastest measurement method among existing unilateral pulse methods. This indicates that, compared to unilateral pulse experimental methods, the use of the congenetic bilateral pulse method can increase the measurement speed by at least four times.

## 5.2. Accuracy analysis

Due to limitations in the precision of measuring instruments or environmental disturbances, there may be errors in the input parameters when calculating the permeability of the sample according to equation (18). The  $\delta X$  defined in this study represents the deviation of the measured value of variable  $X$  from its true value. Utilizing error propagation formulas and equation (18), the relative error in the calculated permeability result can be expressed as:

$$\frac{\delta k_{app}}{k_{app}} = \sqrt{\left(\frac{\delta \beta_p}{\beta_p}\right)^2 + \left(\frac{\delta \mu}{\mu}\right)^2 + \dots} \quad (22)$$

The influence of measurement errors in all input parameters on the final calculated permeability result should be considered theoretically. Nevertheless, in the course of conducting pulse decay experiments via diverse methodologies, the measurement errors associated with parameters such as gas viscosity, compressibility, sample length, and the like exert an equivalent influence on the resultant permeability calculations across all experimental approaches. Consequently, when comparing the accuracy of different experimental approaches, these variables can be temporarily ignored. It is important to note that in equation (18), porosity appears in the numerator, and the denominator contains  $\theta_1$ , which is a function of the ratios of the sample pore volume to the volume of the upstream and downstream chambers ( $V_{uD}$  and  $V_{dD}$ ). The measurement error in the volume of the upstream and downstream chambers is much smaller than the measurement error in sample porosity. Hence, the accuracy of the measurement primarily depends on how sensitive the permeability calculation result is to errors in porosity.

The sensitivity, denoted as  $s$ , is defined as the relative error in permeability calculation results caused by a relative error in unit porosity. According to equation (18), the expression for sensitivity can be written as follows:

$$s = \frac{\partial(\ln k_{app})}{\partial(\ln \varphi)} = 1 - 2 \frac{\partial(\ln \theta_1)}{\partial(\ln \varphi)} \quad (23)$$

Combined with equation (11), the sensitivity  $s$  for different ratios of the upstream and downstream volumes can be calculated. Fig. 6(a) displays the calculated sensitivity  $s$  of permeability calculation results to porosity errors in the congenetic bilateral pulse method. The contour lines of sensitivity in the figure correspond to the contour lines of the sum of the upstream and downstream volumes. As the sum of the upstream and downstream volumes increases, sensitivity initially decreases and then rises again, with a minimum value of approximately 0.6. This implies that in the congenetic bilateral pulse method, adjusting chamber volumes cannot entirely eliminate permeability calculation errors caused by porosity inaccuracies.

According to the above calculations, the sensitivity of the different methods depends on the relationship between the parameter  $\theta_1$  and the volume ratio  $V_{uD}$  and  $V_{dD}$ . The calculated equation of parameter  $\theta_1$  for the conventional pulse decay method can be referred to the article of wang et al.<sup>10</sup> Considering the two-chamber unilateral pulse case,  $\tan \theta_m = (V_{uD} + V_{dD})\theta_m / (\theta_m^2 - V_{uD}V_{dD})$ , the sensitivity cloud of the conventional unilateral pulse method can be obtained by bringing it into equation (23), as shown in Fig. 6(b). When the chambers on both sides are equal ( $V_{uD} = V_{dD}$ ), the sensitivity will eventually decay to 0 as the volume of the chambers on both sides increases ( $V_{uD}$  and  $V_{dD}$  decrease). In particular, when  $V_{uD} = V_{dD} < 0.65$ , there is  $s < 0.1$ , at which point the permeability error due to the porosity error will be an order of magnitude smaller than the porosity error itself. When the volumes of

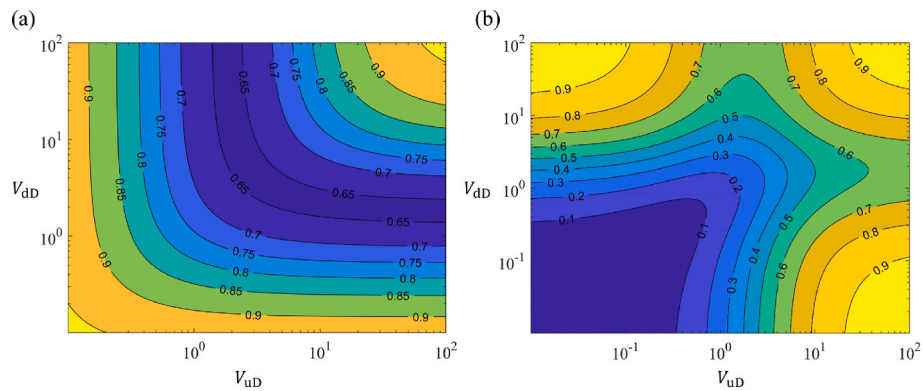


**Fig. 6.** Variation of sensitivity with upstream and downstream volume ratios: (a) The congenetic bilateral pulse method. The minimum sensitivity value is about 0.6. (b) The conventional unilateral pulse decay method. The one-end constant pressure method corresponds to the minimum value of  $V_{uD}$  or  $V_{dD}$ , and the one-end sealed method corresponds to the maximum value of  $V_{uD}$  or  $V_{dD}$ .

the chambers at both sides are unequal ( $V_{uD} \neq V_{dD}$ ), increasing the volume of the relatively smaller side of the chamber will favor a reduction in sensitivity. If the pressure at one side of the sample is kept constant, increasing the volume of the chamber at the other side helps to reduce the sensitivity. When one side of the sample is sealed, the sensitivity is always greater than 0.6 regardless of chamber volume changes. Therefore, the error sensitivity of the bilateral pulse method is consistent with its intrinsic one-end sealed method.

In summary, in comparison to other unilateral pulse experimental methods proposed in existing literature, the congenetic bilateral pulse method presented in this study exhibits a notable enhancement in measurement speed, amounting to a minimum fourfold increase. Regarding the sensitivity of permeability calculation results to porosity errors, since the limited chamber volume method at both ends can be made less sensitive by increasing the upstream and downstream chamber volumes, the congenetic bilateral pulse method is comparable to the one-end sealed experiment while being higher to experiments with limited chamber volumes at both ends of the sample. This suggests that the bilateral pulse method is suitable for applications where measurement speed is crucial and a slight compromise in accuracy can be tolerated.

## 6. Conclusions

This study presents the congenetic bilateral pulse-decay method, which achieves simultaneity and symmetry in applying pulses to both sides of the sample by directly connecting the upstream and downstream chambers through a bypass. Theoretical derivations lead to more concise analytical solutions and permeability calculation processing and experiments verified the feasibility of the method. A comprehensive evaluation method is utilized to analyze measurement duration and error sensitivity. Compared to existing unilateral pulse experimental approaches, the congenetic bilateral pulse method improves measurement speed by at least four times. Furthermore, the sensitivity of permeability calculation results to porosity errors is similar to that of the one-end sealed method but higher than the method with finite volume chambers at both ends of the sample. Consequently, the congenetic bilateral pulse method is suitable for applications that require high measurement speed while allowing for some relaxation in terms of accuracy.

## CRedit authorship contribution statement

**Mingbao Zhang:** Writing – original draft, Validation, Investigation. **Yue Wang:** Data curation. **Zhiguo Tian:** Software, Investigation, Formal analysis. **Moran Wang:** Writing – review & editing, Supervision, Conceptualization.

## Declaration of competing interest

The authors declare that they have no known competing financial interests or personal relationships that could have appeared to influence the work reported in this paper.

## Data availability

No data was used for the research described in the article.

## Acknowledgments

We sincerely appreciate Dr. Gari Gaus and Dr. Bernhard Krooss at RWTH Aachen University for providing the experimental data. This work is financially supported by the NSF grant of China (No. U1837602, 12272207) and the National Key Research and Development Program of China (No. 2019YFA0708704).

## References

- Mukherjee M, Vishal V. Gas transport in shale: a critical review of experimental studies on shale permeability at a mesoscopic scale. *Earth Sci Rev.* 2023;244, 104522.
- Ling K, He J, Pei P, Ge J, Ni X. A method to determine pore compressibility based on permeability measurements. *Int J Rock Mech Min.* 2015;80:51–56.
- Birkholzer J, Houseworth J, Tsang C-F. Geologic disposal of high-level Radioactive waste: status, Key issues, and trends. *Annu Rev Env Resour.* 2012;37(1):79–106.
- Neuzil CE. Permeability of clays and shales. *Annu Rev Earth Pl Sc.* 2019;47(1): 247–273.
- Boot-Handford ME, Abanades JC, Anthony EJ, et al. Carbon capture and storage update. *Energ Environ Sci.* 2014;7(1):130–189.
- Huppert HE, Neufeld JA. The fluid mechanics of carbon dioxide sequestration. *Annu Rev Fluid Mech.* 2014;46(1):255–272.
- Song J, Zhang D. Comprehensive review of caprock-sealing mechanisms for geologic carbon sequestration. *Environ Sci Technol.* 2013;47(1):9–22.
- Lyu Q, Shi J, Pathegama Gamage R. Effects of testing method, lithology and fluid-rock interactions on shale permeability: a review of laboratory measurements. *J Nat Gas Sci Eng.* 2020;78, 103302.
- Sander R, Pan Z, Connell LD. Laboratory measurement of low permeability unconventional gas reservoir rocks: a review of experimental methods. *J Nat Gas Sci Eng.* 2017;37:248–279.
- Wang Y, Tian Z, Nolte S, Amann-Hildenbrand A, Krooss BM, Wang M. Reassessment of transient permeability measurement for tight rocks: the role of boundary and initial conditions. *J Nat Gas Sci Eng.* 2021;95, 104173.
- Wang Y, Liu S, Elsworth D. Laboratory investigations of gas flow behaviors in tight anthracite and evaluation of different pulse-decay methods on permeability estimation. *Int J Coal Geol.* 2015;149:118–128.
- Wang Z, Fink R, Wang Y, Amann-Hildenbrand A, Krooss BM, Wang M. Gas permeability calculation of tight rocks based on laboratory measurements with non-ideal gas slippage and poroelastic effects considered. *Int J Rock Mech Min.* 2018;112: 16–24.
- Chenevert ME, Sharma AK. Permeability and effective pore pressure of shales. *SPE Drill Completion.* 1993;8(1):28–34.
- Heller R, Vermynen J, Zoback M. Experimental investigation of matrix permeability of gas shales. *AAPG Bull.* 2014;98(5):975–995.

15. Yucel Akkutlu I, Fathi E. Multiscale gas transport in shales with local kerogen heterogeneities. *SPE J.* 2012;17(4):1002–1011.
16. Song I, Rathbun AP, Saffer DM. Uncertainty analysis for the determination of permeability and specific storage from the pulse-transient technique. *Int J Rock Mech Min.* 2013;64:105–111.
17. Xu P, Yang S-Q. Permeability evolution of sandstone under short-term and long-term triaxial compression. *Int J Rock Mech Min.* 2016;85:152–164.
18. Alnoaimi KR, Kovscek AR. Influence of microcracks on flow and storage capacities of gas shales at core scale. *Transport Porous Med.* 2019;127(1):53–84.
19. Rushing JA, Newsham KE, Lasswell PM, Cox JC, Blasingame TA. Klinkenberg-corrected permeability measurements in tight gas sands: steady-state versus unsteady-state techniques. In: *SPE Annual Technical Conference and Exhibition. OnePetro.* 2004.
20. Nolte S, Fink R, Krooss BM, et al. Experimental investigation of gas dynamic effects using Nanoporous Synthetic materials as tight rock Analogues. *Transport Porous Med.* 2021;137(3):519–553.
21. Brace WF, Walsh JB, Franjos WT. Permeability of granite under high pressure. *Journal of Geophysical Research (1896-1977).* 1968;73(6):2225–2236.
22. Wang Y, Tian Z, Nolte S, Krooss BM, Wang M. An improved straight-line method for permeability and porosity determination for tight reservoirs using pulse-decay measurements. *J Nat Gas Sci Eng.* 2022;105, 104708.
23. Pan Z, Connell LD. Modelling permeability for coal reservoirs: a review of analytical models and testing data. *Int J Coal Geol.* 2012;92:1–44.
24. Feng R, Liu J, Harpalani S. Optimized pressure pulse-decay method for laboratory estimation of gas permeability of sorptive reservoirs: Part 1 – Background and numerical analysis. *Fuel.* 2017;191:555–564.
25. Hart DJ, Wang HF. A single test method for determination of poroelastic constants and flow parameters in rocks with low hydraulic conductivities. *Int J Rock Mech Min.* 2001;38(4):577–583.
26. Tian Z, Zhang D, Wang Y, Zhou G, Zhang S, Wang M. Inertial solution for high-pressure-difference pulse-decay measurement through microporous media. *J Fluid Mech.* 2023;971, R1.
27. Wang Y, Nolte S, Gaus G, et al. An early-time solution of pulse-decay method for permeability measurement of tight rocks. *J Geophys Res Solid Earth.* 2021;126(12), e2021JB022422.
28. Jones SC. A rapid accurate unsteady-state Klinkenberg permeameter. *SPE J.* 1972;12(5):383–397.
29. Shabani M, Krooss BM, Hallenberger M, Amann-Hildenbrand A, Fink R, Littke R. Petrophysical characterization of low-permeable carbonaceous rocks: comparison of different experimental methods. *Mar Petrol Geol.* 2020;122, 104658.
30. Bourbie T, Walls J. Pulse decay permeability: analytical solution and experimental test. *SPE J.* 1982;22(5):719–721.
31. Chen T, Stagg PW. Semilog analysis of the pulse-decay technique of permeability measurement. *SPE J.* 1984;24(6):639–642.
32. Jin G, Pérez HG, Al Dhamen AA, et al. Permeability measurement of organic-rich shale - comparison of various unsteady-state methods. In: *SPE Annual Technical Conference and Exhibition. SPE.* 2015. D021S017R001.
33. Metwally YM, Sondergeld CH. Measuring low permeabilities of gas-sands and shales using a pressure transmission technique. *Int J Rock Mech Min.* 2011;48(7): 1135–1144.
34. Cui X, Bustin RM, Brezovski R, Nassichuk B, Glover K, Pathi V. A new method to simultaneously measure in-situ permeability and porosity under reservoir conditions: implications for characterization of unconventional gas reservoirs. In: *SPE Canada Unconventional Resources Conference. SPE.* 2010. SPE-138148-MS.
35. Yang Z, Sang Q, Dong M, Zhang S, Li Y, Gong H. A modified pressure-pulse decay method for determining permeabilities of tight reservoir cores. *J Nat Gas Sci Eng.* 2015;27:236–246.
36. Jang H, Lee W, Kim J, Lee J. Novel apparatus to measure the low-permeability and porosity in tight gas reservoir. *J Petrol Sci Eng.* 2016;142:1–12.
37. Hannon MJ. Alternative approaches for transient-flow laboratory-scale permeametry. *Transport Porous Med.* 2016;114(3):719–746.
38. Feng R, Pandey R. Investigation of various pressure transient techniques on permeability measurement of unconventional gas reservoirs. *Transport Porous Med.* 2017;120(3):495–514.
39. Bhandari AR, Flemings PB, Polito PJ, Cronin MB, Bryant SL. Anisotropy and stress dependence of permeability in the barnett shale. *Transport Porous Med.* 2015;108(2): 393–411.
40. Billiotte J, Yang D, Su K. Experimental study on gas permeability of mudstones. *Phys Chem Earth.* 2008;33. Parts A/B/C.
41. Cui X, Bustin AMM, Bustin RM. Measurements of gas permeability and diffusivity of tight reservoir rocks: different approaches and their applications. *Geofluids.* 2009;9(3):208–223.
42. Walder J, Nur A. Permeability measurement by the pulse-decay method: effects of poroelastic phenomena and non-linear pore pressure diffusion. *Int J Rock Mech Min.* 1986;23(3):225–232.